

Analytic calculation of certain scattering parameters from a mode conversion analysis of X-mode–O-mode coupling

C. S. Ng and D. G. Swanson

Physics Department, Auburn University, Auburn, Alabama 36849

(Received 2 May 1994; accepted 10 August 1994)

Certain fast wave scattering parameters from a sixth order mode conversion equation, which represents the coupling of five propagating wave branches in an inhomogeneously magnetized plasma, are shown to be independent of absorption. However, the mode conversion coefficient C_{23} between the X-mode and the O-mode where both propagate in the same direction is not one of these. A recently developed analytical method is applied to calculate C_{23} and one of the nonzero reflection coefficients. Empirical formulas are found for these two coefficients. The result shows that C_{23} is not exactly independent of absorption, but for many cases has an unusually weak dependence. This explains a previous numerical result showing that C_{23} is independent of absorption to numerical accuracy. The coefficient C_{32} is also calculated by the same method and is shown to be equal to C_{23} as required by a proven reciprocity relation. The weak dependence of C_{23} on absorption has to be taken into consideration by any theory that attempts to treat a five branch problem as two separated three branch problems. © 1994 American Institute of Physics.

I. INTRODUCTION

Effects like transmission, reflection, mode conversion and absorption usually exist when a wave propagates in a weakly inhomogeneous medium through a back-to-back resonance-cutoff region. These phenomena can be modeled by different kinds of high order one dimensional ordinary differential equations (called mode conversion equations here). Many of these equations have been derived to study the mode conversion effect between fast waves and slow waves, or between X-mode fast waves and O-mode fast waves, in a weakly inhomogeneously magnetized plasma. This latter case permits some interesting scenarios for accessibility, since at the various electron cyclotron harmonics, there is a region where an X-mode from the low density side encounters first the $R=0$ cutoff and then the upper hybrid resonance, where it again propagates, but this region is effectively inaccessible from the outside (and the outside is inaccessible from the inside). Because of the coupling between the X-mode and the O-mode with finite k_{\parallel} in an inhomogeneous plasma at these harmonics, the region is weakly accessible through mode conversion where both the X-mode and the O-mode are coupled to a Bernstein mode and hence coupled to one another. Without absorption, this coupling can be treated as a two step problem where each of the cold waves are coupled to the Bernstein wave in a standard mode conversion analysis, and then these two results can be cascaded to obtain the coupling between the two cold modes. With absorption, however, the cascading of the two separate mode conversions is more problematical, as an earlier analysis of the unseparated problem, which includes the X-mode, O-mode, and Bernstein mode simultaneously seemed to show that the X-mode–O-mode coupling was independent of absorption^{1,2} whereas the cascaded approach shows strong dependence on absorption. Since the coupling is weak in either case for laboratory plasmas, this effect is probably unimportant for fusion, but for magnetospheric and astrophysical plasmas, this coupling could lead to leakage of

wave energy from a region with either a density maximum or a density minimum where the cold X-mode may be trapped, but the converted O-mode may escape.

Because the full wave coupling models of mode conversion are so complicated, being ordinary differential equations of sixth order for the second harmonic and eighth order for the third harmonic, it is difficult to obtain good numerical results over a wide range of parameters. This paper exploits a new method for including the effects of absorption using only asymptotic methods which result in fast and accurate results for certain coupling coefficients (including the important X-mode–O-mode coefficient), and also proves that several other coefficients are independent of absorption so that analytic results are validated. For the cases where there is only conversion between a single cold wave and a warm wave, the model equation is a fourth order equation of the form (e.g., Refs. 3–8)

$$\psi^{iv} + \lambda^2 z (\psi'' + \psi) + \gamma \psi = h(z) (\psi'' + \psi), \quad (1)$$

where $h(z)$ is the absorption function which must fall off at least as fast as z^{-1} as $|z| \rightarrow \infty$, and with λ and γ being real constants. This equation describes coupling of three branches of propagating waves, two fast wave branches (one on either side, both X-mode or both O-mode) and a slow wave branch on the $z > 0$ side. We call this a three branch problem. An equation that describes coupling of five branches of propagating waves is⁹

$$\begin{aligned} \psi^{vi} + \lambda^2 z [\psi^{iv} + (1 + k_0^2) \psi'' + k_0^2 \psi] + \gamma_2 \psi'' + \gamma_0 \psi \\ = h(z) [\psi^{iv} + (1 + k_0^2) \psi'' + k_0^2 \psi], \end{aligned} \quad (2)$$

where λ , γ_2 , γ_0 and k_0 are real constants. The parameter k_0 is the ratio of the wavelengths of the two fast wave branches as $|z| \rightarrow \infty$ and has been chosen to be always smaller than unity here. The dispersion relation for this equation is

$$-k^6 + \lambda^2 z [k^4 - (1 + k_0^2) k^2 + k_0^2] - \gamma_2 k^2 + \gamma_0.$$

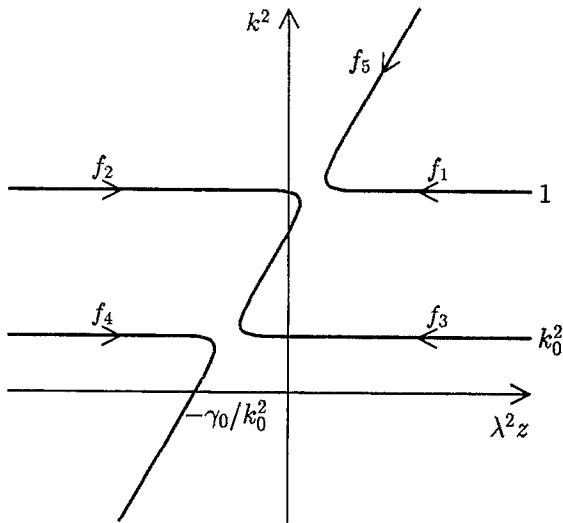


FIG. 1. Schematic plot of the dispersion relation for the + case.

This relation is plotted on Figs. 1 and 2 for two cases, namely $\alpha_2, \alpha_4 > 0$ (+ case) and $\alpha_2, \alpha_4 < 0$ (- case), where

$$\begin{aligned} \alpha_2 &= (1 + \gamma_2 - \gamma_0)/2\lambda^2(1 - k_0^2), \\ \alpha_4 &= (-k_0^6 - \gamma_2 k_0^2 + \gamma_0)/2\lambda^2 k_0(1 - k_0^2). \end{aligned} \quad (3)$$

These two equations can both describe physical situations like second ion cyclotron harmonic and second electron cyclotron harmonic in an inhomogeneously magnetized plasma. It is well known that only the X-mode exists along a direction perpendicular to the magnetic field if the wave frequency ω is smaller than the plasma frequency ω_p . Hence a five branch problem only exists for $\omega > \omega_p$ and it must be a five branch problem whenever the X-mode is propagating

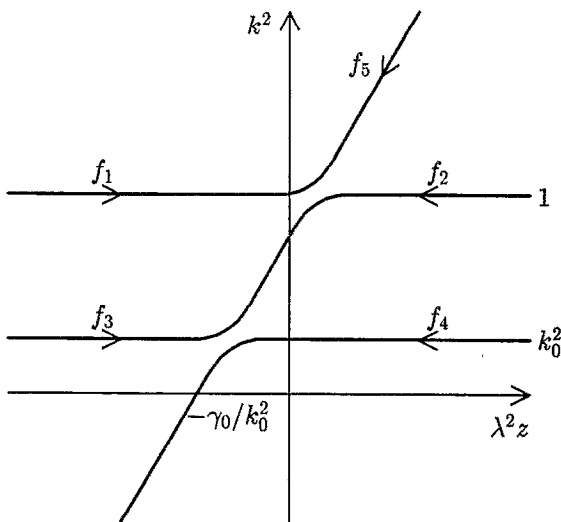


FIG. 2. Schematic plot of the dispersion relation for the - case.

because the O-mode always exists for this case. However, Eq. (1) is frequently used to model the X-mode for all ω . This is because the coupling between X-mode and O-mode is usually weak (especially for small k_{\parallel} , the component of the wave vector along the direction of the magnetic field) and it is sometimes argued that we can treat the five branch problem as two separated three branch problems. Moreover, since it was found that all mode conversion coefficients of a three branch problem tend to zero as absorption increases, the coupling between the X-mode and the O-mode should become vanishingly small when the absorption is strong. Note also that other researchers, using the phase space method to study the mode conversion problem, also believe that multiple mode conversions can be treated individually and combined with the eikonal method if the mode conversion points are separated in phase space.¹⁰

Another mode conversion equation that describes a five branch problem is an eighth order equation^{9,1,2}

$$\begin{aligned} \psi^{iviii} + \gamma_6 \psi^{vi} - \lambda^2 z [\psi^{iv} + (1 + k_0^2) \psi'' + k_0^2 \psi] - \gamma_2 \psi'' - \gamma_0 \psi \\ = h(z) [\psi^{iv} + (1 + k_0^2) \psi'' + k_0^2 \psi], \end{aligned} \quad (4)$$

which can model physical situations like the third ion or electron cyclotron harmonic.

One surprising result from a previous study was that the nonzero mode conversion coefficient C_{23} from Eq. (4) between the X-mode and the O-mode branches propagating in the same direction appeared to be independent of absorption to the numerical accuracy^{2,9} (note that it is called C_{41} in Ref. 2). If this result were true, then there is a great difficulty in understanding this by the separation scheme. The difficulty is that for large absorption, all mode conversion coefficients between fast and slow waves vanish for the two individual three branch problems and it is hard to imagine why the mode conversion coefficient between the two fast modes does not vanish after the two three branch problems are combined into a single five branch problem since the coupling is via an intermediate slow wave. Before we investigate further along this direction, it is better to calculate the same coefficient using other analytical methods to check this numerical result. We will present in detail the theory for Eq. (2) only, but will show that the results from both Eqs. (2) and (4) are very similar.

There is a standard method to calculate all scattering parameters from mode conversion equations like Eqs. (1), (2) or (4) analytically for $h=0$.^{11,12} For $h \neq 0$, there exists a well developed numerical method to calculate solutions and scattering parameters from these equations.^{4,7,2} This method involves solving a "homogeneous equation" (i.e., with $h=0$) by numerical contour integrations and then solving the "inhomogeneous equation" by converting it into an integral equation which is solved iteratively, using the solutions of the former equation to form the kernel. The scattering parameters can then be calculated by numerically integrating an integral involving h and solutions of these two equations.

By considering contours for the solutions of Eq. (1) with $h=0$ for complex z values, Swanson and Shvets were able to show that some of these integrals are identically zero.¹³ Thus, fast wave transmission coefficients from both sides

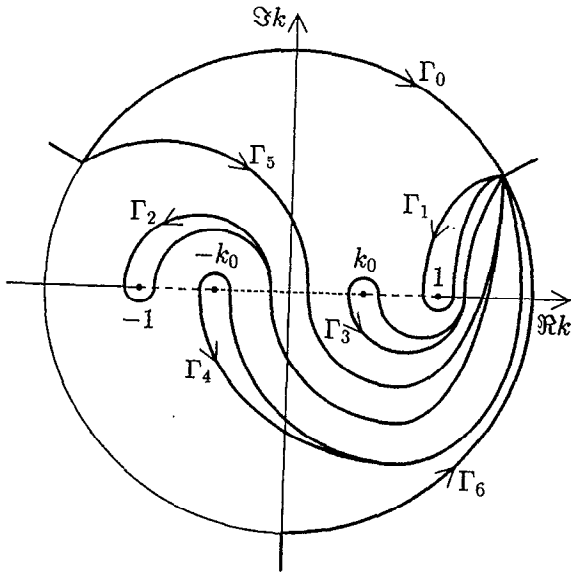


FIG. 3. General contours of f_j 's for the + case.

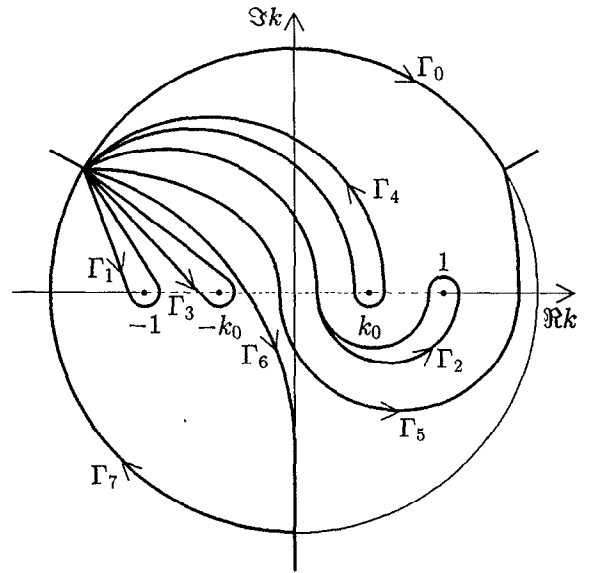


FIG. 4. General contours of f_j 's for the - case.

(which are equal to each other) and the fast wave reflection coefficient from the side which encounters the resonance before the cutoff (which is identically zero), were shown to be independent of absorption. Here we extend this proof to cover Eq. (2) to see if the coefficient C_{23} can also be shown to be independent of absorption. This extension turns out to be not quite straightforward. By this proof, many fast wave scattering parameters are shown to be independent of absorption. However, as we will see, the coefficient C_{23} is not one of them.

We then apply a recently developed analytical method¹⁴ to calculate C_{23} . This method generates an analytic series which can be summed numerically. For completeness, we also try to apply it to calculate other nonzero fast wave scattering parameters. It turns out that this method only works for $C_{23}(C_{32})$ and R_4 which is the nonzero reflection coefficient for the fast wave with the longer wavelength. Empirical formulas are found for both coefficients. From these results, we find that C_{23} is not identically zero, but the dependence on absorption is usually much weaker than for other coefficients when k_0 is close to unity. We will also calculate C_{32} using the series method to see if it is equal to C_{23} as required by the reciprocity relations which have been proved analytically.^{15,2}

In the next section, we will present the integral equations of Eq. (2) for both \pm cases. We will show in Sec. III how to generalize solutions of the "homogeneous equation" for complex z values using contour integrations in the complex k -plane. In Sec. IV, we will be able to see why some scattering parameters are independent of absorption and why some scattering parameters can be calculated by the series method. Numerical results for C_{23} , R_4 and C_{32} will also be presented there. Discussions and conclusions will be presented in Sec. V.

II. INTEGRAL EQUATIONS

The homogeneous equation for Eq. (2) is

$$f^{vi} + \lambda^2 z [f^{iv} + (1 + k_0^2) f'' + k_0^2 f] + \gamma_2 f'' + \gamma_0 f = 0.$$

This equation can be solved exactly by using the method of Laplace:⁸

$$f_j(z) = c_j \int_{\Gamma_j} Q(k)^{-1} [\exp zg(k)] dk, \quad (5)$$

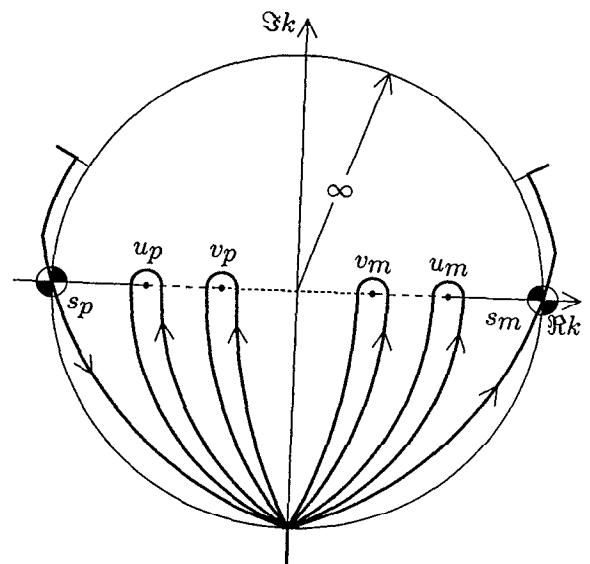


FIG. 5. Topology of the contours for $z \rightarrow \infty \exp(i\theta)$ with $0 \leq \theta < \theta_1$, plotted for $\theta=0$.

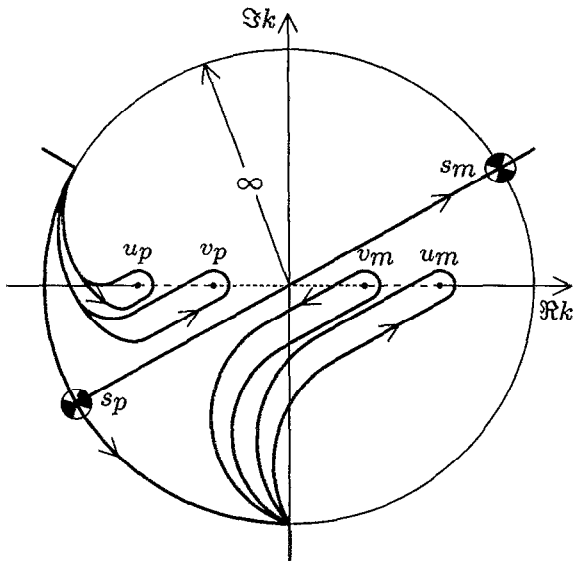


FIG. 6. Topology of the contours for $z \rightarrow \infty \exp(i\theta)$ with $\theta_1 < \theta < \theta_2$, plotted for $\theta = \pi/3$.

where the Γ_j are contours in the complex k -plane which must end at infinity with approach angles of $\pi/6$, $5\pi/6$, or $3\pi/2$, and

$$g(k) = -ik - \frac{i}{z} \left\{ S(k) + \sum_{q=1}^4 \alpha_q \ln(k - k_q) \right\},$$

with

$$S(k) = -[k^3/3 + (1 + k_0^2)k]/\lambda^2, \quad Q(k) = (k^2 - 1)(k^2 - k_0^2), \\ k_1 = -k_2 = 1, \quad k_3 = -k_4 = k_0, \quad \alpha_1 = -\alpha_2, \quad \alpha_3 = -\alpha_4.$$

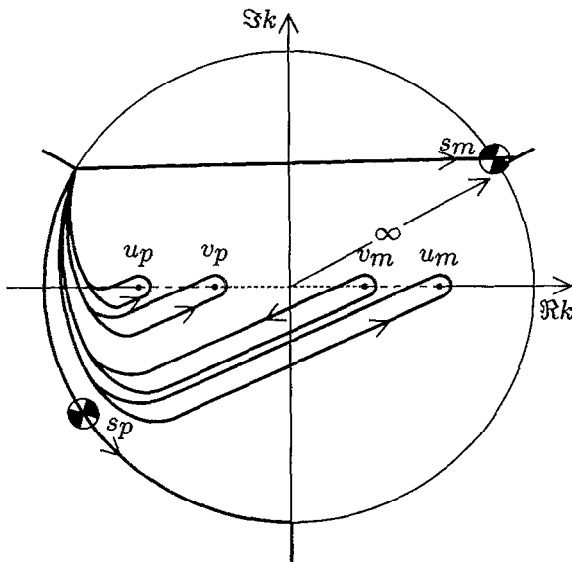


FIG. 7. Topology of the contours for $z \rightarrow \infty \exp(i\theta)$ with $\pi/3 < \theta_2 < \theta < \pi/2 = \theta_3$.

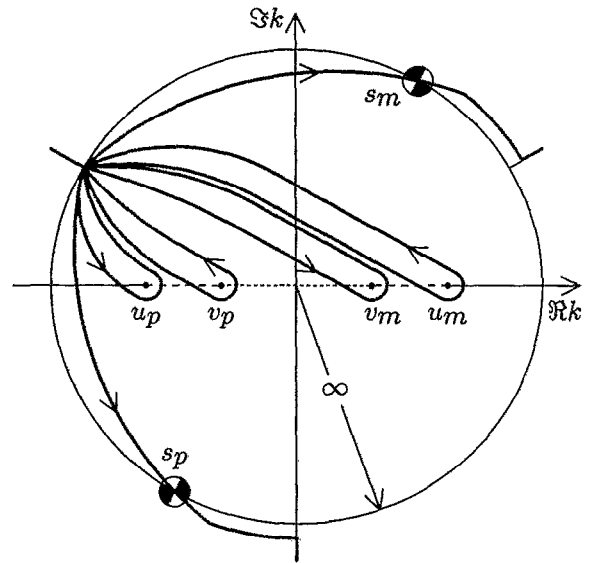


FIG. 8. Topology of the contours for $z \rightarrow \infty \exp(i\theta)$ with $\pi/2 < \theta < \theta_4 > 2\pi/3$, plotted for $\theta = 2\pi/3$.

Note that the corresponding f_j for Eq. (1) is often calculated by integrals in the u -plane, using a transformation $k = i \tan u$ in an equation similar to Eq. (5). The main advantage of working in the u -plane is that there is no branch cut in the u -plane while there is one branch cut from $k=1$ to $k=-1$ for Eq. (1) in the k -plane. However, since there are two branch cuts (the other is from $k=k_0$ to $k=-k_0$) for Eq. (2), we cannot avoid them by introducing the u -plane.

We will only consider the two cases (\pm cases) defined before (see Figs. 1 and 2), and note that the directions of the incident waves of the solutions f_j are indicated by the

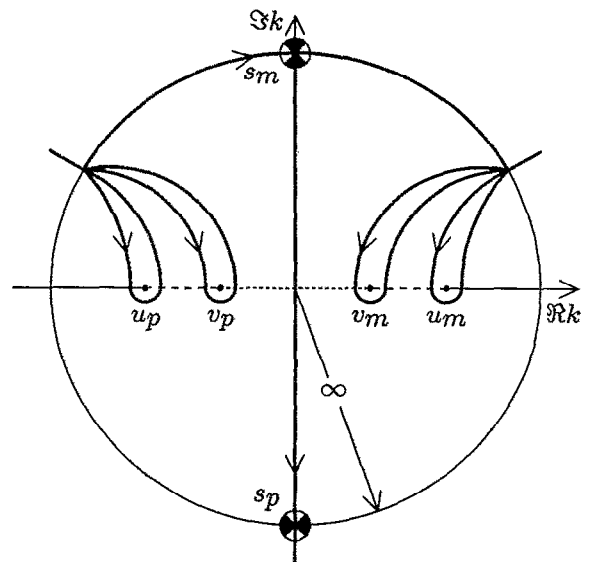


FIG. 9. Topology of the contours for $z \rightarrow \infty \exp(i\theta)$ with $\theta_4 < \theta \leq \pi$, plotted for $\theta = \pi$.

arrows on the curves. The general contours Γ_j for the two cases are shown in Figs. 3 and 4. Figures 5–9 show the contours of asymptotic solutions for some complex z values with $|z| \rightarrow \infty$ for different phase angle θ , where $z = |z|\exp(i\theta)$. We will look at these figures in more detail in

the next section. To find the asymptotic behavior of f_j for real z , we can match these general contours to those contours for $z \rightarrow \pm\infty$ which are shown in Figs. 5 and 9. Then, with a suitable choice of constant c_j , we can express the asymptotic behavior of f_j as

$$\begin{pmatrix} 0 & T_1 & 0 & C_{14} & 0 & C_{16} \\ 1 & R_2 & 0 & C_{24} & 0 & C_{26} \\ 0 & C_{32} & 0 & T_3 & 0 & C_{36} \\ 0 & C_{42} & 1 & R_4 & 0 & C_{46} \\ 0 & C_{52} & 0 & C_{54} & 0 & C_{56} \\ 0 & C_{62} & 0 & C_{64} & 1 & R_6 \end{pmatrix} \begin{pmatrix} u_+ \\ u_- \\ v_+ \\ v_- \\ \sigma_+ \\ \sigma_- \end{pmatrix} \xrightarrow{z \rightarrow \infty} \begin{pmatrix} f_1 \\ f_2 \\ f_3 \\ f_4 \\ f_5 \\ f_6 \end{pmatrix} \xrightarrow{z \rightarrow \infty} \begin{pmatrix} R_1 & 1 & C_{13} & 0 & C_{15} & 0 \\ T_2 & 0 & C_{23} & 0 & C_{25} & 0 \\ C_{31} & 0 & R_3 & 1 & C_{35} & 0 \\ C_{41} & 0 & T_4 & 0 & C_{45} & 0 \\ C_{51} & 0 & C_{53} & 0 & R_5 & 0 \\ C_{61} & 0 & C_{63} & 0 & C_{65} & 1 \end{pmatrix} \begin{pmatrix} u_+ \\ u_- \\ v_+ \\ v_- \\ s_- \\ s_+ \end{pmatrix}, \quad (6)$$

for the + case, and

$$\begin{pmatrix} R_1 & 1 & C_{13} & 0 & 0 & C_{16} \\ T_2 & 0 & C_{23} & 0 & 0 & C_{26} \\ C_{31} & 0 & R_3 & 1 & 0 & C_{36} \\ C_{41} & 0 & T_4 & 0 & 0 & C_{46} \\ C_{51} & 0 & C_{53} & 0 & 0 & C_{56} \\ C_{61} & 0 & C_{63} & 0 & 1 & R_6 \end{pmatrix} \begin{pmatrix} u_- \\ u_+ \\ v_- \\ v_+ \\ \sigma_+ \\ \sigma_- \end{pmatrix} \xrightarrow{z \rightarrow \infty} \begin{pmatrix} f_1 \\ f_2 \\ f_3 \\ f_4 \\ f_5 \\ f_6 \end{pmatrix} \xrightarrow{z \rightarrow \infty} \begin{pmatrix} 0 & T_1 & 0 & C_{14} & C_{15} & 0 \\ 1 & R_2 & 0 & C_{24} & C_{25} & 0 \\ 0 & C_{32} & 0 & T_3 & C_{35} & 0 \\ 0 & C_{42} & 1 & R_4 & C_{45} & 0 \\ 0 & C_{52} & 0 & C_{54} & R_5 & 1 \\ 0 & C_{62} & 0 & C_{64} & C_{65} & 0 \end{pmatrix} \begin{pmatrix} u_- \\ u_+ \\ v_- \\ v_+ \\ s_+ \\ s_- \end{pmatrix}, \quad (7)$$

for the - case, with scattering parameters given by

$$S_{ij} = \begin{pmatrix} R_1 & T_1 & C_{13} & C_{14} & C_{15} & C_{16} \\ T_2 & R_2 & C_{23} & C_{24} & C_{25} & C_{26} \\ C_{31} & C_{32} & R_3 & T_3 & C_{35} & C_{36} \\ C_{41} & C_{42} & T_4 & R_4 & C_{45} & C_{46} \\ C_{51} & C_{52} & C_{53} & C_{54} & R_5 & C_{56} \\ C_{61} & C_{62} & C_{63} & C_{64} & C_{65} & R_6 \end{pmatrix} = S_{ij}^{(0)}, \quad (8)$$

$$S_{ij}^{(0)} = \begin{pmatrix} 0 & T_u & 0 & 0 & -C_u & 0 \\ T_u & T_u^2 C_u^2 & -C_u C_v & T_v C_u C_v & T_u T_v^2 C_u & T_v C_u \\ 0 & -C_u C_v & 0 & T_v & -T_u C_v & 0 \\ 0 & T_v C_u C_v & T_v & C_v^2 & T_u T_v C_v & C_v \\ -C_u & T_u T_v^2 C_u & -T_u C_v & T_u T_v C_v & T_u^2 T_v^2 & T_u T_v \\ 0 & T_v C_u & 0 & C_v & T_u T_v & 1/2 \end{pmatrix}, \quad (8)$$

where $T_u = \exp(-\pi|\alpha_1|)$, $T_v = \exp(-\pi|\alpha_3|)$, $C_u^2 = 1 - T_u^2$, $C_v^2 = 1 - T_v^2$ and the six basic waves types are given asymptotically by

$$u_{\pm} \equiv \frac{\pi \sqrt{T_u} \exp\{\pm i[S(1) - s_u + z + \alpha_2 \ln|z|]\}}{C_u \alpha_1 (1 - k_0^2) \Gamma(\pm i \alpha_2)},$$

$$v_{\pm} \equiv \frac{-\pi \sqrt{T_v} \exp\{\pm i[S(k_0) - s_v + k_0 z + \alpha_4 \ln|z|]\}}{C_v \alpha_3 k_0 (1 - k_0^2) \Gamma(\pm i \alpha_4)},$$

$$s_{\pm} \equiv \frac{\text{sgn}(\alpha_2) \sqrt{\pi}}{\lambda^{7/2} z^{9/4}} \exp\left\{\pm i \left[\frac{2}{3} \lambda z^{3/2} - (1 + k_0^2) \frac{z^{1/2}}{\lambda} - \pi/4 \right]\right\},$$

$$\sigma_+ \equiv \frac{i \sqrt{\pi} e^{\pi(\alpha_1 + \alpha_3)}}{\lambda^{7/2} |z|^{9/4}} \exp\left\{\frac{2}{3} \lambda |z|^{3/2} + (1 + k_0^2) \frac{|z|^{1/2}}{\lambda}\right\},$$

$$\sigma_- \equiv \frac{\text{sgn}(\alpha_2) \sqrt{\pi} e^{\pi(\alpha_2 + \alpha_4)}}{\lambda^{7/2} |z|^{9/4}} \exp\left\{-\frac{2}{3} \lambda |z|^{3/2} - (1 + k_0^2) \frac{|z|^{1/2}}{\lambda}\right\}, \quad (9)$$

with

$$s_u = \alpha_1 \ln 2 + \alpha_3 \ln(1 + k_0/1 - k_0),$$

$$s_v = \alpha_1 \ln(1 + k_0/1 - k_0) + \alpha_3 \ln(2k_0).$$

Note that only f_1 to f_5 are physically allowed in an unbounded region since F_6 is exponentially growing. Using these we can find an integral equation that solves Eq. (2),

$$\begin{aligned} \psi_k = f_k - \frac{f_2 I_{1k}^-}{T_u} - \frac{f_4 I_{3k}^-}{T_v} - \frac{C_u C_v}{T_u T_v} f_4 I_{1k}^- - f_6 I_{0k}^- - \frac{f_1 I_{2k}^+}{T_u} \\ - \frac{f_3 I_{4k}^+}{T_v} - \frac{C_u C_v}{T_u T_v} f_1 I_{4k}^+ - f_0 I_{6k}^+, \quad \text{for the } + \text{ case,} \\ \psi_k = f_k + \frac{f_1 I_{2k}^-}{T_u} + \frac{f_3 I_{4k}^-}{T_v} + \frac{C_u C_v}{T_u T_v} f_1 I_{4k}^- + f_7 I_{0k}^- \\ + \frac{f_2 I_{1k}^+}{T_u} + \frac{f_4 I_{3k}^+}{T_v} + \frac{C_u C_v}{T_u T_v} f_4 I_{1k}^+ + f_0 I_{7k}^+, \end{aligned} \quad (10)$$

for the $-$ case,

where

$$I_{jk}^\pm = \frac{\pm 1}{2\pi i \lambda^2} \int_z^{\pm\infty} F_j(y) h(y) \Psi_k(y) dy,$$

with

$$\begin{aligned} F_j = f_j^{iv} + (1 + k_0^2) f_j'' + k_0^2 f_j, \\ \Psi_j = \psi_j^{iv} + (1 + k_0^2) \psi_j'' + k_0^2 \psi_j, \end{aligned} \quad (11)$$

and $T_u T_v f_0 \equiv f_5 - T_u C_v f_3 - C_u f_1$ for the $+$ case, and $f_0 \equiv T_u T_v f_5 + T_v C_u f_2 + C_v f_4$, $f_7 \equiv f_6 - C_u f_1 / T_u T_v - C_v f_3 / T_v$ for the $-$ case. Note that $f_0 \rightarrow \sigma_-$ as $z \rightarrow -\infty$ for both cases. Equation (10) can be solved iteratively using $\psi_k = f_k$ as the first trial function with f_k calculated numerically by Eq. (5). This can be done for the five physical solutions, $k=1,2,3,4,5$, if $h(z)$ falls off at least as fast as z^{-1} as $|z| \rightarrow \infty$. For the $k=6$ solution, this can be done only if $h(z) \sigma_+(z) \rightarrow 0$ fast enough as $z \rightarrow -\infty$. After solving Eq. (10), scattering parameters can be found, making use of Eqs. (6)–(8), by

$$S_{jk} = S_{jk}^{(0)} \mp I_{kj} = S_{kj}^{(0)} \mp I_{jk}, \quad \text{for } \pm \text{ cases,} \quad (12)$$

with

$$I_{jk} = \frac{1}{2\pi i \lambda^2} \int_{-\infty}^{\infty} F_j(z) h(z) \Psi_k(z) dz, \quad (13)$$

where the second equality in Eq. (12) is by a reciprocity relation $I_{jk} = I_{kj}$ which can be proved from the symmetric properties of the integral equations.² From Eqs. (8) and (12), we see that $S_{jk} = S_{kj}$ is a symmetric matrix. In the Appendix, we show that some of these I_{jk} are identically zero for some kinds of h functions, and thus some scattering parameters are independent of absorption and can be expressed by Eq. (8).

III. SCATTERING PARAMETERS

A. Independence of absorption

By the definition of I_{jk} in Eq. (A1) and the asymptotic behavior of Ψ_k and F_j , described by Eqs. (A8) and (A14), on the contours C_\pm for the two cases, we know immediately that for certain reflection (I_{jj}) and conversion coefficients,

$$I_{11} = I_{33} = I_{13} = I_{31} = I_{14} = I_{41} = 0.$$

Using the fact that on C_\pm , $h \sim \mathcal{O}(|z|^{-1})$, and

$$F_k \sim \mathcal{O}(|z|^{-1} f_k),$$

for $k=1,2,3,4$, by Eqs. (9) and (11), we also know that for all of the fast wave transmission coefficients,

$$I_{12} = I_{21} = I_{34} = I_{43} = 0.$$

Then from the relations of the scattering parameters with I_{jk} in Eq. (12), using Eq. (8), we can find certain fast wave scattering parameters analytically, namely:

$$T_1 = T_2 = T_u, \quad T_3 = T_4 = T_v,$$

$$R_1 = R_3 = C_{13} = C_{31} = C_{14} = C_{41} = 0.$$

Obviously, these scattering parameters are independent of absorption. However, the conversion coefficient $C_{23} (= C_{32})$ which has been found numerically to be independent of absorption is not one of these. So we need to calculate it by another method.

B. Series method

In this section, we will apply a recently developed analytical method to find the series expressions for some of these nonzero fast wave scattering parameters. The correctness of this method has been shown by the very good agreement between the results from the series method and the integral equation method in calculating the nonzero fast wave reflection coefficient from Eq. (1).¹⁴ The derivation here will be very similar to Ref. 14 and we refer to it for details that are omitted here.

Since we need to perform explicit calculations in this section, we need to specify the absorption function h . We will consider two kinds of functions that appear frequently in physical situations. For the nonrelativistic cases, we use

$$h(z) = \lambda^2 \kappa [\zeta \mp 1/Z(\pm \zeta)], \quad (14)$$

for \pm cases, and for relativistic cases from Eq. (2),

$$h(z) = \lambda^2 \kappa [\zeta \pm 1/F_{7/2}(\mp \zeta - 7/2)], \quad (15)$$

and for the relativistic cases from Eq. (4),

$$h(z) = -\lambda^2 \kappa [\zeta \pm 1/F_{9/2}(\mp \zeta - 9/2)], \quad (16)$$

where $Z(\zeta) = i\sqrt{\pi} w(\zeta)$ is the plasma dispersion function, and w is the error function for complex argument,¹⁶ and F_q is the relativistic plasma dispersion function,^{17,18} and $\zeta = (z - z_0)/\kappa$, where κ is a real parameter characterizing the strength of absorption. Note that $Z(\zeta)$, $F_{7/2}(\zeta)$ and $F_{9/2}(\zeta)$ are analytic functions and have zeros only in the lower half ζ -plane. We will also assume that $z_0 = -\gamma_0/k_0^2 \lambda^2$, which is often the case for physical situations. We refer to Refs. 1, 2, and 9 for the dependence on plasma parameters of the dimensionless parameters λ^2 , γ_6 , γ_2 , γ_0 , k_0 , and κ . In the calculations here, we will use these dimensionless parameters as inputs so that the conclusions are not restricted to a particular physical situation.

First we need to expand $h(z)$ in an asymptotic series over C_\pm for the two cases,

$$h(z) \rightarrow \sum_{n=1}^{\infty} \frac{h_n}{y^n}.$$

We have already shown a general method to do so, for those functions of Eqs. (14)–(16), in Ref.14.

For the mode conversion coefficient $C_{23} = -C_u C_v \mp I_{32}$, for the \pm cases, we have, by Eq. (A1) and the asymptotic behavior of Eqs. (A3)–(A13),

$$\begin{aligned} I_{32} &= \frac{1}{2\pi i \lambda^2} \int_{C_{\pm}} F_3(z) h(z) \Psi_2(z) dz, \\ &= \frac{1}{2\pi i \lambda^2} \int_{C_+} F_{vm}(y) h(y) \Psi_{up}(y) dy, \quad \text{for + case,} \\ &= \frac{1}{2\pi i \lambda^2} \int_{C_-} F_{vp}(y) h(y) \Psi_{um}(y) dy, \quad \text{for - case,} \end{aligned} \quad (17)$$

where $y = z - z_0$ and

$$\begin{aligned} \Psi_{up}(y) &\equiv T_u c_u \sum_{n=1}^{\infty} \frac{\alpha_{un}}{y^n} e^{i(y + \alpha_2 \ln y)}, \\ \Psi_{um}(y) &\equiv c_u^* \sum_{n=1}^{\infty} \frac{\alpha_{un}^*}{y^n} e^{-i(y + \alpha_2 \ln y)}, \\ F_{vp}(y) &\equiv T_v c_v \sum_{n=1}^{\infty} \frac{\tilde{\alpha}_{vn}}{y^n} e^{i(k_0 y + \alpha_4 \ln y)}, \\ F_{vm}(y) &\equiv c_v^* \sum_{n=1}^{\infty} \frac{\tilde{\alpha}_{vn}^*}{y^n} e^{-i(k_0 y + \alpha_4 \ln y)}, \end{aligned} \quad (18)$$

with c_u, c_v being the coefficients of u_+ and v_+ in Eqs. (9),

$$\begin{aligned} c_u &= \frac{\pi \sqrt{T_u} \exp\{i[S(1) - s_u + z_0]\}}{C_u \alpha_1 (1 - k_0^2) \Gamma(i\alpha_2)}, \\ c_v &= \frac{\pi \sqrt{T_v} \exp\{i[S(k_0) - s_v + k_0 z_0]\}}{C_v \alpha_4 k_0 (1 - k_0^2) \Gamma(i\alpha_4)}. \end{aligned}$$

Similarly, we can calculate the mode conversion coefficient $C_{32} = -C_u C_v \mp I_{23}$, with

$$\begin{aligned} I_{23} &= \frac{1}{2\pi i \lambda^2} \int_{C_{\pm}} F_2(z) h(z) \Psi_3(z) dz, \\ &= \frac{1}{2\pi i \lambda^2} \int_{C_+} F_{up}(y) h(y) \Psi_{vm}(y) dy, \quad (+ \text{ case}), \\ &= \frac{1}{2\pi i \lambda^2} \int_{C_-} F_{um}(y) h(y) \Psi_{vp}(y) dy, \quad (- \text{ case}), \end{aligned} \quad (19)$$

where the definitions of $F_{up}, F_{um}, \Psi_{vp}$, and Ψ_{vm} are similar to Eqs. (18),

$$\Psi_{vp}(y) \equiv T_v c_v \sum_{n=1}^{\infty} \frac{\alpha_{vn}}{y^n} e^{i(k_0 y + \alpha_4 \ln y)},$$

$$\Psi_{vm}(y) \equiv c_v^* \sum_{n=1}^{\infty} \frac{\alpha_{vn}^*}{y^n} e^{-i(k_0 y + \alpha_4 \ln y)},$$

$$F_{up}(y) \equiv T_u c_u \sum_{n=1}^{\infty} \frac{\tilde{\alpha}_{un}}{y^n} e^{i(y + \alpha_2 \ln y)},$$

$$F_{um}(y) \equiv c_u^* \sum_{n=1}^{\infty} \frac{\tilde{\alpha}_{un}^*}{y^n} e^{-i(y + \alpha_2 \ln y)}. \quad (20)$$

From Eqs. (A3)–(A13), we also see that we can calculate the reflection coefficient $R_4 = C_v^2 \mp I_{44}$ by the series method, with

$$\begin{aligned} I_{44} &= \frac{1}{2\pi i \lambda^2} \int_{C_{\pm}} F_4(z) h(z) \Psi_4(z) dz, \\ &= \frac{1}{2\pi i \lambda^2} \int_{C_+} F_{vp}(y) h(y) \Psi_{vp}(y) dy, \quad (+ \text{ case}), \\ &= \frac{1}{2\pi i \lambda^2} \int_{C_-} F_{vm}(y) h(y) \Psi_{vm}(y) dy, \quad (- \text{ case}). \end{aligned} \quad (21)$$

However, we also see that the series method is not able to calculate the coefficients $R_2 = T_v^2 C_u^2 \pm I_{22}$ and $C_{24} = C_{42} = T_v C_u C_v \pm I_{42}$. The reason is that by Eqs. (A3)–(A13), $f_2 \propto v_p + u_p$ for $-\pi/2 < \theta < 0$ on C_+ and $f_2 \propto v_m + u_m$ for $\pi/2 < \theta < \pi$ on C_- . It is obvious that the contributions from the v_p or v_m terms to I_{22} or I_{42} cannot be proved to be zero so that, e.g.

$$\begin{aligned} I_{22} &\neq \frac{1}{2\pi i \lambda^2} \int_{C_+} F_{up}(z) h(z) \Psi_{up}(z) dz, \\ I_{42} &\neq \frac{1}{2\pi i \lambda^2} \int_{C_+} F_{vp}(z) h(z) \Psi_{up}(z) dz, \end{aligned} \quad (22)$$

for the + case. Moreover, we do not know how to calculate these contributions since v_p or v_m only appear on half of a semicircle. There is another reason that, as we will see, even if Eq. (22) were true, the series from the right hand sides are found to be divergent numerically.

To calculate the coefficients α_{un} and α_{vn} , we can substitute the asymptotic series of Ψ_{up} , and Ψ_{vp} of Eqs. (18) and (20), making use of Eq. (11), into Eq. (2), requiring that all terms vanish. The result for α_{un} is

$$\alpha_{un} = a_{n,4} - (1 + k_0^2) a_{n,2} + k_0^2 a_{n,0}, \quad n \geq 1, \quad (23a)$$

$$\begin{aligned} a_{n,0} &= \frac{1}{2i\lambda^2(1 - k_0^2)n} \left\{ [\alpha_2 + i(n-1)] \left[\sum_{m=0}^5 a_{n-1,m} \right. \right. \\ &\quad \left. \left. - \lambda^2 z_0 \alpha_{un} - \lambda^2 (\alpha_2 + in) \right. \right. \\ &\quad \left. \left. \times [a_{n-1,2} + 2a_{n-1,1} + (2 - k_0^2) a_{n-1,0}] \right. \right. \\ &\quad \left. \left. + \gamma_2 (a_{n-1,1} + a_{n-1,0}) \right] + \sum_{m=1}^{n-1} h_{n-m} \alpha_{um} \right\}, \end{aligned} \quad (23b)$$

$$a_{n,k} = a_{n,k-1} + [\alpha_2 + i(n-1)] a_{n-1,k-1}, \quad k = 1, 2, 3, 4, 5, \quad (23c)$$

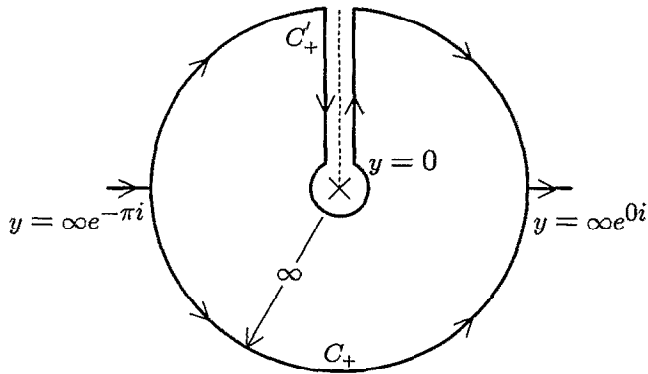


FIG. 10. Integration contours on the complex plane for the + case.

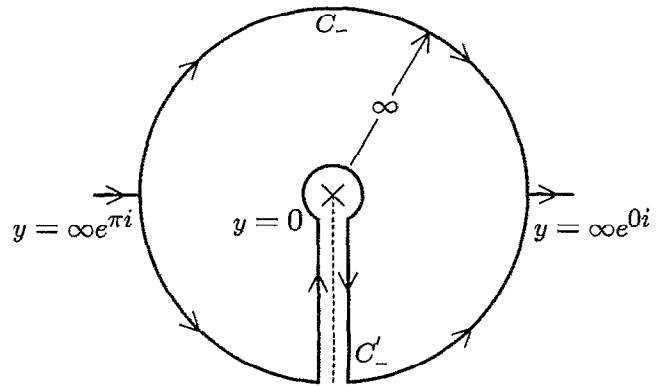


FIG. 11. Integration contours on the complex plane for the - case.

and $a_{0,k} = 1$. We can also use Eqs. (23a)–(23c) to calculate $\tilde{\alpha}_{un}$ by putting $h_n = 0$.

Similarly for α_{vn} ,

$$\alpha_{vn} = a_{n,4} - (1 + k_0^2)a_{n,2} + k_0^2 a_{n,0}, \quad n \geq 1, \quad (24a)$$

$$a_{n,0} = \frac{1}{2i\lambda^2 k_0 (k_0^2 - 1)n} \left\{ [\alpha_4 + i(n-1)] \left[\sum_{m=0}^5 k_0^{5-m} a_{n-1,m} - \lambda^2 z_0 \alpha_{vn} - \lambda^2 (\alpha_4 + in) [a_{n-1,2} + 2k_0 a_{n-1,1} + (2k_0^2 - 1)a_{n-1,0}] + \gamma_2 (a_{n-1,1} + k_0 a_{n-1,0}) \right] + \sum_{m=1}^{n-1} h_{n-m} \alpha_{vm} \right\}, \quad (24b)$$

$$a_{n,k} = a_{n,k-1} + [\alpha_4 + i(n-1)] a_{n-1,k-1}, \quad k = 1, 2, 3, 4, 5, \quad (24c)$$

and $a_{0,k} = 1$. Similarly we use Eqs. (24a)–(24c) to calculate $\tilde{\alpha}_{vn}$ with $h_n = 0$.

Now that we have an exact asymptotic expansion of the integrands of Eqs. (17)–(21), we can write down the series expressions for those integrals, making use of the result

$$I_n^\pm = \int_{C_\pm} \frac{dy}{y^n} e^{\pm i(\delta y + \Delta \ln y)} = 2\pi e^{\pi\Delta/2} \delta^{n-1} e^{\pm i\Delta} (\pm i)^n / \Gamma(n \mp i\Delta),$$

for real $\delta > 0$, where we have changed the contours of integration from C_\pm to C'_\pm in Figs. 10 and 11, using Hankel's contour integral Eq. (A2).

We finally have, for the + case,

$$R_4 = C_v^2 + \frac{i\pi^2 T_v^2 e^{2i[S(k_0) - s_v + k_0 z_0]}}{2\lambda^2 \alpha_4^2 k_0^3 (1 - k_0^2)^2 C_v^2 \Gamma^2(i\alpha_4)} (2k_0)^{2i\alpha_4} \times \sum_{n=3}^{\infty} \frac{\gamma_n (2ik_0)^n}{\Gamma(n + 2i\alpha_3)},$$

$$C_{23} = -C_u C_v - \frac{i\pi^2 T_u T_v e^{i[S(1) - S(k_0) - s_u + s_v + (1 - k_0)z_0]}}{\lambda^2 \alpha_2 \alpha_4 k_0 (1 - k_0^2)^2 C_u C_v \Gamma(i\alpha_2) \Gamma(i\alpha_3)} \times (1 - k_0)^{i(\alpha_1 - \alpha_3) - 1} \sum_{n=3}^{\infty} \frac{\gamma_n [i(1 - k_0)]^n}{\Gamma[n + i(\alpha_1 - \alpha_3)]}, \quad (25)$$

where γ_n is the coefficient of the y^{-n} terms of the integrand after combining the three series from F, Ψ , and h ,

$$\gamma_n = \sum_{m=1}^{n-2} \beta_{n-m} h_m, \quad n \geq 3,$$

$$\beta_n = \sum_{m=1}^{n-1} \alpha_{u(n-m)} \tilde{\alpha}_{vm}^*, \quad n \geq 2, \quad \text{for } C_{23},$$

$$\beta_n = \sum_{m=1}^{n-1} \alpha_{v(n-m)} \tilde{\alpha}_{vm}, \quad n \geq 2, \quad \text{for } R_4. \quad (26)$$

The series for the - case is formally the complex conjugate of Eq. (25), but may have different h_n . The series for the coefficient C_{32} is also formally identical to the C_{23} series in Eq. (25) with only a change of β_n in Eq. (26) to

$$\beta_n = \sum_{m=1}^{n-1} \tilde{\alpha}_{u(n-m)} \alpha_{vm}^*.$$

Note that we can also calculate the three corresponding coefficients for the eighth order equation (4) using Eq. (25) with the sign of the second term (the term with the summation) of both expressions changed to the opposite. But now, instead of Eq. (3),

$$\alpha_2 = (1 - \gamma_6 + \gamma_2 - \gamma_0) / 2\lambda^2 (1 - k_0^2),$$

$$\alpha_4 = (-k_0^8 + \gamma_6 k_0^6 - \gamma_2 k_0^2 + \gamma_0) / 2\lambda^2 k_0 (1 - k_0^2),$$

and

$$S(k) = - \left\{ \frac{k^5}{5} + \frac{(1+k_0^2-\gamma_6)k^3}{3} + [(1-\gamma_6)(1+k_0^2)+k_0^4]k \right\} / \lambda^2.$$

Also, $a_{n,0}$ in Eqs. (23b) and (24b) have to be calculated by slightly more complicated recurrence formulas respectively,

$$a_{n,0} = \frac{1}{2i\lambda^2(1-k_0^2)n} \left\{ [\alpha_2 + i(n-1)] \times \left[\sum_{m=0}^7 a_{n-1,m} - \gamma_6 \sum_{m=0}^5 a_{n-1,m} - \lambda^2 z_0 \alpha_{un} - \lambda^2 (\alpha_2 + in)[a_{n-1,2} + 2a_{n-1,1} + (2-k_0^2)a_{n-1,0}] + \gamma_2(a_{n-1,1} + a_{n-1,0}) \right] - \sum_{m=1}^{n-1} h_{n-m} \alpha_{um} \right\},$$

$$a_{n,0} = \frac{1}{2i\lambda^2 k_0 (k_0^2 - 1)n} \left\{ [\alpha_4 + i(n-1)] \left[\sum_{m=0}^7 k_0^{7-m} a_{n-1,m} - \gamma_6 \sum_{m=0}^5 k_0^{5-m} a_{n-1,m} - \lambda^2 z_0 \alpha_{vn} - \lambda^2 (\alpha_4 + in) \times [a_{n-1,2} + 2k_0 a_{n-1,1} + (2k_0^2 - 1)a_{n-1,0}] + \gamma_2(a_{n-1,1} + k_0 a_{n-1,0}) \right] + \sum_{m=1}^{n-1} h_{n-m} \alpha_{vm} \right\},$$

where the first equation replaces Eq. (23b) and the second equation replaces Eq. (24b).

Let us consider the nonrelativistic case using Eq. (14) as the h function first. The series for C_{23} in Eq. (25) is then evaluated numerically. Since the asymptotic series of h for both \pm cases are the same, the C_{23} values from both cases are simply complex conjugate to each other so that the absolute values of them are identical. An empirical formula is found for it from numerical results,

$$|C_{23}|^2 \approx C_u^2 C_v^2 e^{-(1-k_0)^2 \kappa^2 / 2}, \quad (27)$$

for small $|\alpha_2|$, $|\alpha_4|$, not too small λ^2 and not too large κ . However, the series is not uniformly convergent. One radius of convergence is numerically found to be $k_0 > 1/3$ (note again that k_0 has been chosen to be smaller than unity always), independent of other parameters. The analytical reason for this divergence is not clear for now, but it is found that this radius is not very clear cut. For not too small k_0 and not too large κ , the series first converges to a value expected by the empirical formula Eq. (27) and then diverges away. In examining the convergence of a similar series for a three branch problem, it was found that the convergence radius in κ was a function of machine precision, so it is believed that the apparent divergence in κ is not fundamental, and that the series is probably absolutely convergent in κ . The dependence of the radius of convergence on k_0 is different, however, and may truly represent a finite range of k_0 over which

TABLE I. Nonrelativistic case with $\lambda^2=20$, $|\alpha_2|=0.12$, $|\alpha_4|=0.001$, and $\kappa=2$. Note that $P_0=0.3317\%$.

| k_0 | n | P_{32} | P_{23} | P'_{23} | q_{23} | q'_{23} |
|-------|-----|----------|----------|-----------|----------|-----------|
| 0.1 | 8 | 0.0618 | 0.0618 | 0.0627 | 1.0376 | 1.0280 |
| 0.2 | 8 | 0.0914 | 0.0914 | 0.0921 | 1.0067 | 1.0012 |
| 0.3 | 23 | 0.1258 | 0.1258 | 0.1262 | 0.9892 | 0.9860 |
| 0.4 | 157 | 0.1627 | 0.1627 | 0.1630 | 0.9890 | 0.9867 |
| 0.5 | 152 | 0.2023 | 0.2023 | 0.2025 | 0.9886 | 0.9870 |
| 0.6 | 147 | 0.2417 | 0.2417 | 0.2418 | 0.9882 | 0.9870 |
| 0.7 | 140 | 0.2776 | 0.2776 | 0.2777 | 0.9878 | 0.9868 |
| 0.8 | 132 | 0.3065 | 0.3065 | 0.3065 | 0.9873 | 0.9866 |
| 0.9 | 119 | 0.3252 | 0.3252 | 0.3252 | 0.9867 | 0.9863 |
| 0.95 | 109 | 0.3300 | 0.3300 | 0.3300 | 0.9863 | 0.9861 |
| 0.99 | 90 | 0.3316 | 0.3316 | 0.3316 | 0.9860 | 0.9860 |
| 0.999 | 72 | 0.3317 | 0.3317 | 0.3317 | 0.9860 | 0.9860 |

the series converges. In Tables I and II, some values of $P_{23} \equiv 100|C_{23}|^2$ are shown, along with the values of q_{23} which is defined by $P_{23} = 100P_0 \exp[-q_{23}(1-k_0)^2 \kappa^2 / 2]$, with $P_0 \equiv C_u^2 C_v^2$. Note that q_{23} equals to unity if the empirical formula Eq. (27) gives the exact value. The values n in Table I is the number of terms summed in the evaluation of the series Eq. (25). For those values with $k_0 < 1/3$, we stop the evaluation at a term which has the smallest difference between the values if one more (or less) term is summed, because of the divergence problem. The n values for those data in Table II is from 150 to 153, but remain the same for each line of data. Note also that not all digits shown on these tables are significant figures. Only those digits without an underbar remain unchanged if one more (or less) term is summed. These nonconvergent figures are shown in order to compare the convergence properties with other series.

One obvious quantity to be compared with C_{23} is the C_{32} coefficient, because mathematically it should be identical to C_{23} so that if the values from the series of these two differ with each other, we know they cannot both be correct. This may indicate that neither of the values are truly converged or that there are other errors. So we also show the values of $P_{32} \equiv 100|C_{32}|^2$ in Tables I and II. The values of q_{32} defined similarly as q_{23} are also shown in Table II. We

TABLE II. Nonrelativistic case with $\lambda^2=200$, $|\alpha_2|=0.12$, $|\alpha_4|=0.001$, and $k_0=0.5$. Note that $P_0=0.3317\%$.

| κ | P_{32} | P_{23} | P'_{23} | q_{32} | q_{23} | q'_{23} |
|----------|-----------|----------|-----------|----------|----------|-----------|
| 0.1 | 0.3312 | 0.3312 | 0.3312 | 0.9904 | 0.9904 | 0.9903 |
| 0.5 | 0.3216 | 0.3216 | 0.3216 | 0.9903 | 0.9903 | 0.9902 |
| 1 | 0.2930 | 0.2930 | 0.2931 | 0.9902 | 0.9902 | 0.9900 |
| 2 | 0.2022 | 0.2022 | 0.2022 | 0.9894 | 0.9894 | 0.9892 |
| 4 | 4.622e-2 | 4.622e-2 | 4.625e-2 | 0.9853 | 0.9853 | 0.9851 |
| 6 | 4.148e-3 | 4.148e-3 | 4.157e-3 | 0.9737 | 0.9736 | 0.9732 |
| 8 | 1.801e-4 | 1.803e-4 | 1.818e-4 | 0.9398 | 0.9397 | 0.9386 |
| 10 | 6.603e-6 | 6.694e-6 | 6.830e-6 | 0.8660 | 0.8649 | 0.8632 |
| 12 | 2.560e-7 | 2.843e-7 | 2.918e-7 | 0.7819 | 0.7761 | 0.7746 |
| 14 | 7.887e-9 | 1.522e-8 | 1.556e-8 | 0.7165 | 0.6897 | 0.6888 |
| 16 | 1.916e-10 | 3.434e-9 | 3.454e-9 | 0.6647 | 0.5746 | 0.5744 |
| 18 | 4.419e-12 | 3.787e-9 | 3.787e-9 | 0.6183 | 0.4516 | 0.4516 |
| 20 | 2.831e-11 | 6.346e-9 | 6.248e-9 | 0.4637 | 0.3554 | 0.3557 |
| 22 | 345.3 | 345.3 | 345.3 | -0.1148 | -0.1148 | -0.1148 |

see that the two quantities P_{23} and P_{32} are identical to each other when $k_0 \geq 0.3$ and $\kappa < 10$. The deviation for small k_0 is obviously due to the divergence problem of the series. Also, when κ starts to grow larger, we know from calculations that the terms in the series grow to large values and then decrease, but at the same time the coefficient tends to zero. Since we can only compute it using finite precision and only a finite number of terms can be summed, we know that the series must effectively diverge beyond some large κ value. The fact that P_{23} and P_{32} in Table II do not get smaller for $\kappa > 18$ shows the error is starting to get large so that the values before that may also not have fully converged to the true values due to the subtraction errors. This can be seen by the fact that $P_{23} \neq P_{32}$ for $12 < \kappa$. One interesting fact is that P_{23} agrees with P_{32} again after the series obviously has encountered numerical difficulties (see the values at $\kappa=22$). Being different from the divergence problem for small k_0 , this error is only numerical and there probably does not exist a finite radius of convergence in κ .

Another quantity to compare with is the C_{23} coefficient from the eighth order equation (4). The values of P'_{23} and q'_{23} , defined similarly, are also shown in Tables I and II. We see that the values of P'_{23} , q'_{23} are very close to P_{23} and q_{23} respectively, even for those values that are not fully converged. This shows that the two series have very similar convergence properties. This agreement is also found to be true for cases with different parameters. Obviously, the empirical formula Eq. (27) is also valid for this case.

An empirical formula is also found for R_4 ,

$$|R_4|^2 \approx C_v^4 e^{-2k_0^2 \kappa^2},$$

for small $|\alpha_2|$, $|\alpha_4|$, not too small λ^2 and not too large κ . This empirical formula is consistent with that for R_2 of the fourth order equation (1), $|R_2|^2 \approx C^4 \exp(-2\kappa^2)$, since as $|\alpha_2| \rightarrow 0$, the five branch problem represented by Eq. (2) becomes a three branch problem represented by Eq. (1) and then $R_4 \rightarrow R_2$ with $k_0 \kappa \rightarrow \kappa$. However, the radius of convergence for this series is $k_0 < 1/3$, just opposite to that of the series of C_{23} . For k_0 larger and near $1/3$, the series also first apparently converges to a certain reasonable value and then diverges away.

Let us now consider the relativistic case by using Eqs. (15) as the h function. Since now the h function for the \pm cases are slightly different, we will do our calculation mainly on the $-$ case. The empirical formula for C_{32} is now

$$|C_{23}|^2 \approx C_u^2 C_v^2 e^{-7(1-k_0)^2 \kappa^2 / 2}. \quad (28)$$

The radius of convergence $k_0 > 1/3$ is the same for this case, but now there is another radius of convergence $(1-k_0)\kappa < 1$, similar to the radius of convergence $\kappa < 0.5$ for R_2 from Eq. (1) for the relativistic case. Some values of P_{23} , and q_{23} , which is now defined by $P_{23} = 100P_0 \exp[-q_{23}^2 7(1-k_0)^2 \kappa^2 / 2]$, are shown in Tables III and IV. Note that this empirical formula Eq. (28) also works for the $+$ case. Actually, it works even slightly better than the $-$ case. The values of C_{23} are generally close for the two cases. The q_{23} values for the $+$ case, which we call q_{23}^+ , are also shown in Table III.

TABLE III. Relativistic case with $\lambda^2=100$, $|\alpha_2|=0.12$, $|\alpha_4|=0.001$, and $\kappa=0.6$. Note that $P_0=0.3317\%$.

| k_0 | n | P_{23} | P'_{23} | q_{23} | q'_{23} | q_{23}^+ |
|-------|-----|----------|-----------|----------|-----------|------------|
| 0.1 | 8 | 0.1313 | 0.0985 | 0.9082 | 0.9249 | 0.9922 |
| 0.2 | 15 | 0.1657 | 0.1364 | 0.8606 | 0.8573 | 0.9253 |
| 0.3 | 31 | 0.1923 | 0.1649 | 0.8824 | 0.8799 | 0.9447 |
| 0.35 | 159 | 0.2062 | 0.1803 | 0.8929 | 0.8907 | 0.9532 |
| 0.4 | 157 | 0.2202 | 0.1961 | 0.9030 | 0.9012 | 0.9610 |
| 0.5 | 152 | 0.2480 | 0.2284 | 0.9222 | 0.9210 | 0.9744 |
| 0.6 | 146 | 0.2744 | 0.2600 | 0.9397 | 0.9389 | 0.9845 |
| 0.7 | 140 | 0.2976 | 0.2886 | 0.9551 | 0.9546 | 0.9909 |
| 0.8 | 131 | 0.3159 | 0.3115 | 0.9681 | 0.9679 | 0.9934 |
| 0.9 | 119 | 0.3276 | 0.3264 | 0.9785 | 0.9784 | 0.9918 |
| 0.95 | 108 | 0.3306 | 0.3303 | 0.9826 | 0.9825 | 0.9894 |
| 0.99 | 90 | 0.3316 | 0.3316 | 0.9853 | 0.9853 | 0.9867 |
| 0.999 | 72 | 0.3317 | 0.3317 | 0.9859 | 0.9859 | 0.9860 |

We also did calculations on C_{32} for both cases. The values of C_{23} and C_{32} agree whenever the series converge. We did not show C_{32} and q_{32} in Tables III and IV because they are simply the same as C_{23} and q_{23} .

The empirical formula for R_4 for this case is

$$|R_4|^2 \approx C_v^4 e^{-14k_0^2 \kappa^2},$$

for small $|\alpha_2|$, $|\alpha_4|$, not too small λ^2 and not too large κ . This empirical formula is also consistent with that for R_2 from Eq. (1), $|R_2|^2 \approx C^4 \exp(-14\kappa^2)$.

The values of P'_{23} and q'_{23} calculated by using Eq. (16) as the h function for the eighth order equation (4), are also shown in Tables III and IV. Because of the difference in the h function, the empirical formula for this case becomes

$$|C_{23}|^2 \approx C_u^2 C_v^2 e^{-9(1-k_0)^2 \kappa^2 / 2}. \quad (29)$$

As a result, the P'_{23} values in Tables III and IV are generally different from the P_{23} values, but still q'_{23} are very close to q_{23} , where q'_{23} is now defined by $P'_{23} = 100P_0 \exp[-q'_{23}^2 9(1-k_0)^2 \kappa^2 / 2]$. If we use the negative of Eq. (15) as the h function instead, and calculate P''_{23} and

TABLE IV. Relativistic case with $\lambda^2=100$, $|\alpha_2|=0.12$, $|\alpha_4|=0.001$, $k_0=0.9$, and $n=119$. Note that $P_0=0.3317\%$.

| κ | P_{23} | P_{23}' | P_{23}'' | q_{23} | q_{23}'' | q_{23}^+ |
|----------|----------|-----------|------------|----------|------------|------------|
| 0.6 | 0.3276 | 0.3276 | 0.3264 | 0.9785 | 0.9784 | 0.9784 |
| 0.8 | 0.3245 | 0.3245 | 0.3225 | 0.9749 | 0.9748 | 0.9747 |
| 1.0 | 0.3206 | 0.3206 | 0.3175 | 0.9709 | 0.9708 | 0.9707 |
| 1.2 | 0.3159 | 0.3159 | 0.3115 | 0.9666 | 0.9664 | 0.9664 |
| 1.35 | 0.3119 | 0.3119 | 0.3065 | 0.9631 | 0.9629 | 0.9628 |
| 1.5 | 0.3075 | 0.3075 | 0.3010 | 0.9594 | 0.9592 | 0.9591 |
| 1.6 | 0.3044 | 0.3044 | 0.2971 | 0.9568 | 0.9567 | 0.9565 |
| 1.8 | 0.2977 | 0.2977 | 0.2887 | 0.9514 | 0.9512 | 0.9511 |
| 2.0 | 0.2905 | 0.2905 | 0.2798 | 0.9457 | 0.9455 | 0.9453 |
| 2.2 | 0.2829 | 0.2829 | 0.2703 | 0.9396 | 0.9394 | 0.9391 |
| 2.5 | 0.2706 | 0.2706 | 0.2554 | 0.9300 | 0.9298 | 0.9294 |
| 3.0 | 0.2488 | 0.2488 | 0.2293 | 0.9125 | 0.9123 | 0.9117 |
| 3.5 | 0.2261 | 0.2261 | 0.2028 | 0.8935 | 0.8933 | 0.8924 |
| 4.5 | 0.1813 | 0.1814 | 0.1528 | 0.8520 | 0.8517 | 0.8501 |
| 6.0 | 0.1234 | 0.1234 | 0.0935 | 0.7846 | 0.7844 | 0.7816 |
| 8.0 | 0.06999 | 0.07004 | 0.0454 | 0.6945 | 0.6942 | 0.6903 |

q_{23}'' defined similarly to P_{23} and q_{23} , even the values of P_{23}'' will be very close to those of P_{23} as can be seen from Table IV. This shows that the convergence properties of the two series from the sixth and eighth order equations are very similar. Similarly, the empirical formula for R_4 for this case is,

$$|R_4|^2 \approx C_v^4 e^{-18k_0^2 \kappa^2}.$$

We see that the factor before κ^2 in these empirical formulas depend on the h function rather than the order of the equation, namely the factors are 7 and 14 if we use $F_{7/2}$ or 9 and 18 when we use $F_{9/2}$.

The fact that the C_{23} series diverges for $k_0 < 1/3$ and the R_4 series diverges for $k_0 > 1/3$ makes it very difficult to get both values for the same k_0 accurately, except for k_0 near $1/3$. Although we do not understand this divergence analytically, we may try to see how the $k_0 = 1/3$ limit comes about by looking at the two series in Eq. (25). Note that the n th term of the series of C_{23} is proportional to $(1 - k_0)^n$ and that of R_4 is proportional to $(2k_0)^n$. These two factors $1 - k_0$, and $2k_0$ are equal when $k_0 = 1/3$. From this we can also see another reason why we cannot calculate R_2 and C_{24} by the series method. In order to calculate them, we must evaluate the series from the right hand side of Eq. (22). It is obvious that the n th term of these two series is proportional to 2 and $1 + k_0$ respectively, which are larger than $2/3$ for all k_0 . So these two series are expected to be seriously divergent. Indeed we found that it is so numerically. Therefore, it seems that we cannot calculate R_2 and C_{24} by the series method, at least in the present formulation.

From these empirical formulas (27) to (29) of C_{23} and other numerical results, we see that although C_{23} is not exactly independent of absorption, the dependence is much weaker than other coefficients because of the $(1 - k_0)^2/4$ factor, if k_0 is close to unity. Note that the empirical formula for R_2 should be proportional to $\exp(-2\kappa^2)$, for the nonrelativistic case, similar to that of Eq. (1), but C_{23} is only proportional to $\exp[-(1 - k_0)^2 \kappa^2/2]$. Note also that the factor $C_u^2 C_v^2$ is usually very small for a plasma, since the O-mode transmission coefficient is usually very close to unity so that one of the factors C_u or C_v is very small, depending on which one represents the O-mode. Therefore, when calculating the coefficient C_{23} from solving the integral equation numerically, usually only one or two significant figures can be obtained for realistic cases. Due to the weak dependence on absorption, these one or two significant figures remain unchanged even after other scattering parameters have decayed to relatively small values. Another factor is that the numerical method that solves the integral equation also does not converge for large κ . Thus, it is hard to see how C_{23} changes for really large absorption using that method. That explains why the previous result indicated that C_{23} is independent of absorption,^{2,9} since the k_0 values used there were all close to unity.

IV. DISCUSSION

Although subject to some divergence problems, the series method once again shows its power in calculating fast

wave scattering parameters. We now know that it works for equations with order higher than four and for five branch problems as well as three branch problems. It has been used to calculate C_{23} , the coupling coefficient between the X-mode and the O-mode, for situations with even stronger absorption, with much higher accuracy and efficiency than solving the integral equations numerically. This enables us to conclude definitely that the X-mode-O-mode coupling does depend on absorption and we have found empirical formulas for it for different absorption functions. From these results, we know that the dependence on absorption is usually weak so that we can explain why this dependence was not found by the previous study. It should be noted that while the coupling between the X-mode and the O-mode from branches 2 to 3 or vice versa is nonzero for $k_{\parallel} \neq 0$, the coupling between branches 1 and 4, which represent the same waves traveling in the opposite direction, vanishes identically so the coupling is unidirectional.

The dependence of C_{23} on absorption indeed satisfies the separation scheme for very strong absorption. Since the mode conversion coefficients of the two separated three branch problems all vanish for very strong absorption, the conversion coefficient C_{23} between the two must also vanish eventually. However, because of the weak dependence on absorption of C_{23} , it may not change much for moderately strong absorption, even when the mode conversion coefficients of the two separated problems all become very small. This means that the separation scheme still does not work very well here, not until the absorption becomes extremely strong. This is a fact that must be taken into consideration by any theory that treats the five branch problem as two separated three branch problems. This also shows that solving these higher order equations for the five branch problem may provide more advantages than the separation scheme, even for moderately strong absorption. The example given here has demonstrated that the weak dependence of C_{23} , found by solving these higher order equations numerically will be difficult to emulate using the separation scheme. The affirmation of the weak dependence of the X-mode-O-mode coupling on absorption does give one confidence that analytic expressions (with or without the empirical formulas) for the coupling are unusually robust, and may be used for such plasma wave trapping scenarios mentioned in the introduction over a broad range of parameters.

ACKNOWLEDGMENT

Work supported by U.S. Department of Energy Grant No. DE-FG05-85ER53206-93.

APPENDIX: SOLUTIONS FOR COMPLEX z

One possible way to evaluate I_{jk} of Eq. (13) is to perform the integration in the complex z -plane. This can be done only if the h function has some good analytical properties in the z -plane. We will assume that h is analytic and tends to zero at least as fast as $|z|^{-1}$ for z on or below (above) the real axis for the + (-) case. Note that all the physical situations we consider here satisfy these assumptions. Also, it has been shown that F_j and Ψ_j are analytic

everywhere.¹³ Then we can change the path of integration of I_{jk} , defined as the semicircles C_{\pm} in Figs. 10 and 11,

$$I_{jk} = \frac{1}{2\pi i \lambda z} \int_{C_{\pm}} F_j(z) h(z) \Psi_k(z) dz, \quad (\text{A1})$$

with $y \equiv z - z_0$ on the figures for later convenience. The solutions f_j for complex z values are still defined by Eq. (5) with the same integration contours. The asymptotic behavior of the f_j on C_{\pm} can be found by considering the contours of asymptotic solutions for $z \rightarrow \infty \exp i\theta$, with $-\pi < \theta < 0$ for the + case and $0 < \theta < \pi$ for the - case, see Figs. 10 and 11. Let us look at the - case first. After some consideration, one realizes that there are five regions of θ where these contours are topologically different. These five regions are $0 \leq \theta < \theta_1$, $\theta_1 < \theta < \theta_2$, $\pi/3 < \theta_2 < \theta < \pi/2 \equiv \theta_3$, $\theta_3 < \theta < \theta_4 > 2\pi/3$, and $\theta_4 < \theta \leq \pi$, see Figs. 5-9. The exact values of θ_1 to θ_4 are not important to the proof here except the fact that $\theta_4 > 2\pi/3$, which can be quite obviously seen from these figures. Note that the asymptotic solutions indicated on these figures have the following asymptotic behavior,

$$\begin{aligned} u_p &\propto e^{iz} \downarrow, & u_m &\propto e^{-iz} \uparrow, \\ v_p &\propto e^{ik_0 z} \downarrow, & v_m &\propto e^{-ik_0 z} \uparrow, \\ s_p &\propto e^{i(2/3)\lambda z^{3/2}} \begin{cases} \downarrow & 0 < \theta < 2\pi/3, \\ \uparrow & 2\pi/3 < \theta < \pi, \end{cases} \\ s_m &\propto e^{-i(2/3)\lambda z^{3/2}} \begin{cases} \uparrow & 0 < \theta < 2\pi/3, \\ \downarrow & 2\pi/3 < \theta < \pi, \end{cases} \end{aligned}$$

where \uparrow indicates that it is an exponentially growing solution and \downarrow indicates that it is an exponentially decaying solution.

The circles on these figures, with the four quarters being black and white alternatively, indicate the saddle points of the two slow wave asymptotic solutions. The white quarters represent the downhill sides and the black quarters represent the uphill sides. The positions of these two saddle points for $z = |z| \exp(i\theta)$ are

$$k_s = \pm \lambda z^{1/2} = \pm \lambda |z|^{1/2} e^{i\theta/2},$$

with crossing angles ϕ determined by

$$2\phi + \frac{\theta}{2} = \pm \frac{\pi}{2}.$$

Note that ϕ of each circle on these figures is just the angle of the middle line that divides the circle into two symmetric parts along the two white quarters. We see that the slow wave saddle points tend to infinity as $|z| \rightarrow \infty$, i.e., for z on the contour C_- .

The fast wave asymptotic solutions can be calculated by using Hankel's contour integral,¹⁶

$$\int_{C_H} (e^{-i\pi t})^{-z} e^{-t} dt = -\frac{2\pi i}{\Gamma(z)}, \quad (\text{A2})$$

where the contour C_H starts at $t = \infty \exp(0i)$, comes along the positive real axis, turns around the origin counterclockwise, then goes back along the positive real axis to

$t = \infty \exp(2\pi i)$. The contour of each fast wave has to go around a fast wave branch point k_q , $q=1,2,3$, or 4, that comes in along a direction on which

$$k - k_q = |k - k_q| e^{-i\theta - i\pi/2},$$

and goes out along a direction on which

$$k - k_q = |k - k_q| e^{-i\theta + 3i\pi/2}.$$

These directions are also indicated by the shape of the fast wave contours on Figs. 5-9. This means that these four fast wave contours have to turn 180° as θ changes from 0 to π .

By comparing the topology of the general contours in Fig. 4 to those contours in Figs. 5-9, we can find out the asymptotic behavior of f_j . For $0 < \theta < \theta_1$ (see Fig. 5),

$$\begin{aligned} f_1 &\propto s_p \rightarrow u_p \rightarrow -s_p \propto u_p \downarrow, \\ f_2 &\propto s_p \rightarrow -u_p \rightarrow -v_p \rightarrow u_m \rightarrow v_p \rightarrow u_p \rightarrow -s_p \propto u_m \uparrow, \\ f_3 &\propto s_p \rightarrow -u_p \rightarrow v_p \rightarrow u_p \rightarrow -s_p \propto v_p \downarrow, \\ f_4 &\propto s_p \rightarrow -u_p \rightarrow -v_p \rightarrow v_m \rightarrow v_p \rightarrow u_p \rightarrow -s_p \propto v_m \uparrow, \\ f_5 &\propto s_p \rightarrow -u_p \rightarrow -v_p \rightarrow s_m \propto s_m \uparrow, \\ f_7 &\propto -s_p \downarrow, \\ f_0 &\propto s_p \rightarrow -u_p \rightarrow -v_p \rightarrow -v_m \rightarrow -u_m \rightarrow s_m \propto s_m \uparrow, \end{aligned} \quad (\text{A3})$$

where the \rightarrow indicates the order of going through these paths so that the contours of the individual solutions will be added up to be topologically equal to the the general contour for each solution f_j . We did not show proportional constants which are not important in the discussion here, although they are important in getting the scattering parameters of Eqs. (6)-(8). For $\theta_1 < \theta < \theta_2$ (see Fig. 6),

$$\begin{aligned} f_1 &\propto u_p \downarrow, \\ f_2 &\propto -u_p \rightarrow -v_p \rightarrow s_p \rightarrow u_m \rightarrow -s_p \rightarrow v_p \rightarrow u_p \propto u_m \uparrow, \\ f_3 &\propto -u_p \rightarrow v_p \rightarrow u_p \propto v_p \downarrow, \\ f_4 &\propto -u_p \rightarrow -v_p \rightarrow s_p \rightarrow v_m \rightarrow -s_p \rightarrow v_p \rightarrow u_p \propto v_m \uparrow, \\ f_5 &\propto -u_p \rightarrow -v_p \rightarrow s_p \rightarrow u_m \rightarrow v_m \rightarrow -s_p/2 \rightarrow s_m \propto s_m \uparrow, \\ f_7 &\propto -s_p \downarrow, \\ f_0 &\propto -u_p \rightarrow -v_p \rightarrow s_p/2 \rightarrow s_m \propto s_m \uparrow. \end{aligned} \quad (\text{A4})$$

For $\pi/3 < \theta_2 < \theta < \pi/2 \equiv \theta_3$ (see Fig. 7),

$$\begin{aligned} f_1 &\propto u_p \downarrow, \\ f_2 &\propto -u_p \rightarrow -v_p \rightarrow u_m \rightarrow v_p \rightarrow u_p \propto u_m, \\ f_3 &\propto -u_p \rightarrow v_p \rightarrow u_p \propto v_p \downarrow, \\ f_4 &\propto -u_p \rightarrow -v_p \rightarrow v_m \rightarrow v_p \rightarrow u_p \propto v_m \uparrow, \\ f_5 &\propto -u_p \rightarrow -v_p \rightarrow u_m \rightarrow v_m \rightarrow v_p \rightarrow u_p \rightarrow s_m \propto s_m \uparrow, \\ f_7 &\propto -s_p \downarrow, \\ f_0 &\propto s_m \uparrow. \end{aligned} \quad (\text{A5})$$

For $\theta_3 < \theta < \theta_4$ (see Fig. 8),

$$f_1 \propto u_p \downarrow,$$

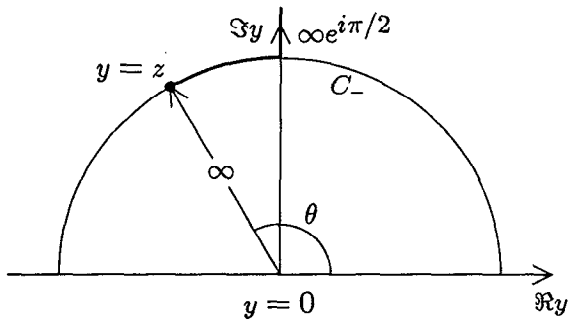


FIG. 12. Integration contours on the complex plane for some of the $I_{jk}^+(z)$ of fast waves for the - case.

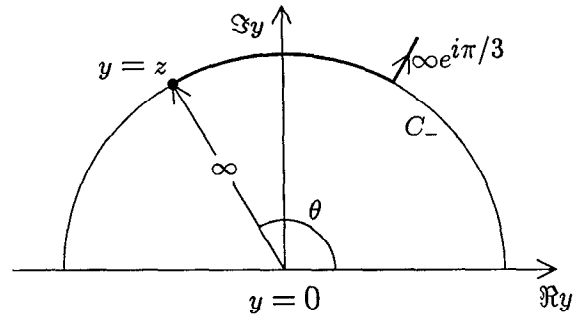


FIG. 13. Integration contours on the complex plane of $I_{jk}^+(z)$ for $k=1,2,3,4$ of the - case.

$$\begin{aligned}
 f_2 &\propto v_m \rightarrow u_m \rightarrow -v_m \propto v_m + u_m \uparrow, \\
 f_3 &\propto v_p \downarrow, \\
 f_4 &\propto v_m \uparrow, \\
 f_5 &\propto v_m \rightarrow u_m \rightarrow s_m \propto \begin{cases} s_m \uparrow & \theta < 2\pi/3, \\ u_m \uparrow & \theta > 2\pi/3, \end{cases} \\
 f_7 &\propto -s_p \begin{cases} \downarrow & \theta < 2\pi/3, \\ \uparrow & \theta > 2\pi/3, \end{cases} \\
 f_0 &\propto s_m \begin{cases} \uparrow & \theta < 2\pi/3, \\ \downarrow & \theta > 2\pi/3. \end{cases} \quad (A6)
 \end{aligned}$$

For $\theta_4 < \theta < \pi$ (see Fig. 9),

$$\begin{aligned}
 f_1 &\propto u_p \downarrow, \\
 f_2 &\propto s_m \rightarrow v_m \rightarrow u_m \rightarrow -v_m \rightarrow -s_m \propto v_m + u_m \uparrow, \\
 f_3 &\propto v_p \downarrow, \\
 f_4 &\propto s_m \rightarrow v_m \rightarrow -s_m \propto v_m \uparrow, \\
 f_5 &\propto s_m \rightarrow v_m \rightarrow u_m \propto u_m \uparrow, \\
 f_7 &\propto -s_p \rightarrow -s_m/2 \rightarrow -v_p \rightarrow -u_p \propto -s_p \uparrow, \\
 f_0 &\propto s_m \downarrow. \quad (A7)
 \end{aligned}$$

In summary, the asymptotic behavior of the fast wave solutions f_1 to f_4 for z on the contours C_- are

$$\begin{aligned}
 f_1 &\propto u_p \propto e^{iz} \downarrow, \\
 f_2 &\propto u_m \propto e^{-iz} \uparrow, \\
 f_3 &\propto v_p \propto e^{ik_0 z} \downarrow, \\
 f_4 &\propto v_m \propto e^{-ik_0 z} \uparrow. \quad (A8)
 \end{aligned}$$

By Eq. (11), it is obvious that F_j has the same asymptotic behavior as f_j . To show that ψ_j , and thus Ψ_j has the same asymptotic behavior as f_j , we need to define ψ_j for complex z values using the integral equation (10). By redefining the end points of some of the integrals in Eq. (10), namely end points of $I_{41}^-, I_{11}^+, I_{31}^+, I_{13}^+, I_{33}^+, I_{14}^+$ changed to $\infty e^{i\pi/2}$ (see Fig. 12), and end points of I_{7k}^+ with $k=1,2,3,4$ changed to $\infty e^{i\pi/3}$ (see Fig. 13), it can be shown that the ψ_k in the left

hand side of Eq. (10) will have the same asymptotic behavior as f_k , provided that the Ψ_k on the right hand side of Eq. (10) is assumed to have this property. This can be seen by considering the asymptotic behavior of each term of the right hand side of Eq. (10) for each k . Note that these redefinitions of end points will not affect the values of ψ_k for z on the real axis. So, Ψ_k indeed has the same asymptotic behavior as f_k , for $k=1,2,3,4$, if the integral equation (10) is convergent for these solutions. This will be true if $h \rightarrow 0$ at least as fast as $|z|^{-1}$, as assumed. Note that the fact that $f_7 \propto s_p$ and $f_0 \propto s_m$ for z on C_- has been used in this proof.

For the + case, the integration contour is changed to C_+ defined in Fig. 10. There are also five regions of θ where the contours of the asymptotic solutions are topologically different. These five regions are $0 \geq \theta > -\theta_1$, $-\theta_1 > \theta > \theta_2$, $-\theta_2 > \theta > -\theta_3$, $-\theta_3 > \theta > -\theta_4$, and $-\theta_4 > \theta \geq -\pi$. The contours for this case are symmetric to those in Figs. 5-9, so we will not show them here, but will point out an easy way to get them from these figures. We only need to make a mirror reflection about the imaginary k -axis of those contours in Figs. 5-9, then exchange the labels $m \leftrightarrow p$, and change the directions of the arrows to the opposite. Then the asymptotic behavior of f_k can be found for each region. For $0 > \theta > -\theta_1$,

$$\begin{aligned}
 f_1 &\propto -s_m \rightarrow u_m \rightarrow s_m \propto u_m \downarrow, \\
 f_2 &\propto -s_m \rightarrow v_p \rightarrow u_p \rightarrow -v_p \rightarrow -v_m \rightarrow s_m \propto v_p + u_p \uparrow, \\
 f_3 &\propto -s_m \rightarrow v_m \rightarrow s_m \propto v_m \downarrow, \\
 f_4 &\propto -s_m \rightarrow v_p \rightarrow s_m \propto v_p \uparrow, \\
 f_5 &\propto s_p \rightarrow -v_p \rightarrow -u_p \rightarrow s_m \propto s_p \uparrow, \\
 f_6 &\propto s_m \downarrow, \\
 f_0 &\propto s_p \rightarrow -u_p \rightarrow -v_p \rightarrow -v_m \rightarrow -u_m \rightarrow s_m \propto s_p \uparrow. \quad (A9)
 \end{aligned}$$

For $-\theta_1 > \theta > -\theta_2$,

$$\begin{aligned}
 f_1 &\propto u_m \downarrow, \\
 f_2 &\propto -s_m \rightarrow v_p \rightarrow u_p \rightarrow -v_p \rightarrow -s_m \propto v_p + u_p \uparrow, \\
 f_3 &\propto v_m \downarrow, \\
 f_4 &\propto -s_m \rightarrow v_p \rightarrow s_m \propto v_p \uparrow,
 \end{aligned}$$

$$\begin{aligned}
f_5 \propto s_p \rightarrow s_m/2 \rightarrow s_p \propto s_p \uparrow, \\
f_6 \propto s_m \downarrow, \\
f_0 \propto s_p \rightarrow s_m/2 \rightarrow -v_m \rightarrow -u_m \propto s_p \uparrow.
\end{aligned}
\tag{A10}$$

For $-\theta_2 > \theta > -\theta_3$,

$$\begin{aligned}
f_1 \propto u_m \downarrow, \\
f_2 \propto v_p \rightarrow u_p \rightarrow -v_p \propto v_p + u_p \uparrow, \\
f_3 \propto v_m \downarrow, \\
f_4 \propto v_p \uparrow, \\
f_5 \propto s_p \rightarrow u_m \rightarrow v_m \rightarrow s_p \propto s_p \uparrow, \\
f_6 \propto s_m \downarrow, \\
f_0 \propto s_p \uparrow.
\end{aligned}
\tag{A11}$$

For $-\theta_3 > \theta > -\theta_4$,

$$\begin{aligned}
f_1 \propto u_m \downarrow, \\
f_2 \propto -u_m \rightarrow -v_m \rightarrow u_p \rightarrow v_m \rightarrow u_m \propto u_p \uparrow, \\
f_3 \propto -u_m \rightarrow v_m \rightarrow u_m \propto v_m \downarrow, \\
f_4 \propto -u_m \rightarrow -v_m \rightarrow v_p \rightarrow v_m \rightarrow u_m \propto v_p \uparrow, \\
f_5 \propto s_p \rightarrow v_m \rightarrow u_m \propto \begin{cases} s_p \uparrow & \theta > -2\pi/3, \\ v_m \downarrow & \theta < -2\pi/3, \end{cases} \\
f_6 \propto s_m \begin{cases} \downarrow & \theta > -2\pi/3, \\ \uparrow & \theta < -2\pi/3, \end{cases} \\
f_0 \propto s_p \begin{cases} \uparrow & \theta > -2\pi/3, \\ \downarrow & \theta < -2\pi/3. \end{cases}
\end{aligned}
\tag{A12}$$

For $-\theta_4 > \theta > -\pi$,

$$\begin{aligned}
f_1 \propto u_m \downarrow, \\
f_2 \propto -u_m \rightarrow -v_m \rightarrow -s_p \rightarrow u_p \rightarrow s_p \rightarrow v_m \rightarrow u_m \propto u_p \uparrow,
\end{aligned}$$

$$\begin{aligned}
f_3 \propto -u_m \rightarrow v_m \rightarrow u_m \propto v_m \downarrow, \\
f_4 \propto -u_m \rightarrow -v_m \rightarrow -s_p \rightarrow v_p \rightarrow s_p \rightarrow v_m \rightarrow u_m \propto v_p \uparrow, \\
f_5 \propto s_p \rightarrow v_m \rightarrow u_m \propto v_m \downarrow, \\
f_6 \propto s_m \rightarrow s_p/2 \rightarrow v_m \rightarrow u_m \propto s_m \uparrow, \\
f_0 \propto s_p \downarrow.
\end{aligned}
\tag{A13}$$

In summary, the asymptotic behavior of the fast wave solutions f_1 to f_4 for z on the contours C_+ are

$$\begin{aligned}
f_1 &\propto u_m \propto e^{-iz} \downarrow, \\
f_2 &\propto u_p \propto e^{iz} \uparrow, \\
f_3 &\propto v_m \propto e^{-ik_0 z} \downarrow, \\
f_4 &\propto v_p \propto e^{ik_0 z} \uparrow.
\end{aligned}
\tag{A14}$$

Using similar arguments, it can be shown that F_k and Ψ_k have the same asymptotic behavior as f_k , for $k=1,2,3,4$.

- ¹J. L. Hu and D. G. Swanson, *Phys. Fluids B* **5**, 4207 (1993).
- ²J. L. Hu and D. G. Swanson, *Phys. Fluids B* **5**, 4221 (1993).
- ³N. S. Erokhin and S. S. Moiseev, *Reviews of Plasma Physics* (Consultants Bureau, New York, 1979), Vol. 7, p. 181.
- ⁴D. G. Swanson, *Nucl. Fusion* **20**, 428 (1980).
- ⁵P. L. Colestock and R. J. Kashuba, *Nucl. Fusion* **23**, 763 (1983).
- ⁶T. H. Stix and D. G. Swanson, *Handbook of Plasma Physics*, edited by A. A. Galeev and R. N. Sudan (North-Holland, Amsterdam, 1983), Vol. 1, p. 335.
- ⁷D. G. Swanson, *Phys. Fluids* **28**, 2645 (1985).
- ⁸D. G. Swanson, *Plasma Waves* (Academic, Boston, 1989).
- ⁹J. Hu, Ph.D. Dissertation, Auburn University, Auburn, Alabama, 1993.
- ¹⁰R. G. Littlejohn and W. G. Flynn, *Phys. Rev. Lett.* **70**, 1799 (1993).
- ¹¹D. J. D. Gambier and J. P. M. Schmitt, *Phys. Fluids* **26**, 2200 (1983).
- ¹²D. J. Gambier and D. G. Swanson, *Phys. Fluids* **28**, 145 (1985).
- ¹³D. G. Swanson and V. F. Shvets, *J. Math. Phys.* **34**, 69 (1993).
- ¹⁴C. S. Ng and D. G. Swanson, *Phys. Plasmas* **1**, 815 (1994).
- ¹⁵S. Cho and D. G. Swanson, *Phys. Fluids B* **2**, 2704 (1990).
- ¹⁶M. Abramowitz and I. Stegun, *Handbook of Mathematical Functions* (National Bureau of Standards, Washington, DC, 1964).
- ¹⁷I. P. Shkarofsky, *Phys. Fluids* **9**, 561 (1966).
- ¹⁸P. A. Robinson, *J. Math. Phys.* **30**, 2484 (1989).